Finite-Time Command-Filtered Composite Adaptive Neural Control of Uncertain Nonlinear Systems

Jinlin Sun, Haibo He, *Fellow, IEEE*, Jianqiang Yi, *Senior Member, IEEE*, and Zhiqiang Pu

***Abstract*—This article presents a new command-filtered composite adaptive neural control scheme for uncertain nonlinear systems. Compared with existing works, this approach focuses on achieving finite-time convergent composite adaptive control for the higher-order nonlinear system with unknown nonlinearities, parameter uncertainties, and external disturbances. First, radial basis function neural networks (NNs) are utilized to approximate the unknown functions of the considered uncertain nonlinear system. By constructing the prediction errors from the serial–parallel nonsmooth estimation models, the prediction errors and the tracking errors are fused to update the weights of the NNs. Afterward, the composite adaptive neural backstepping control scheme is proposed via nonsmooth command filter and adaptive disturbance estimation techniques. The proposed control scheme ensures that high-precision tracking performances and NN approximation performances can be achieved simultaneously. Meanwhile, it can avoid the singularity problem in the finite-time backstepping framework. Moreover, it is proved that all signals in the closed-loop control system can be convergent in finite time. Finally, simulation results are given to illustrate the effectiveness of the proposed control scheme.**

***Index Terms*—Adaptive control, backstepping, command filter, finite-time control, neural networks (NNs).**

I. Introduction

BACKSTEPPING technique is a typical control tool for higher-order nonlinear systems and it has attracted wide attention as the technique presents a systematic recursive design framework for tracking and regulation control [1]–[6]. Nevertheless, in the traditional backstepping design process, the repeated analytic differentiation of virtual control laws is needed, which results in the problem of "explosion of complexity." To eliminate this problem, dynamic surface control (DSC) [7] was proposed by letting virtual control laws pass through linear filters. Furthermore, a command-filtered backstepping control [8], [9] was presented to avoid analytic differentiation and remove the filtering errors caused by filters simultaneously.

Although these modified backstepping control methods are applicable for uncertain nonlinear systems theoretically, they need large enough gains to suppress uncertainties, which may lead to saturation problems and degrade closed-loop performances [10]–[12]. For the nonlinear systems with high uncertainties, fuzzy-logic systems [13]–[15] and neural networks (NNs) [16]–[22] can be employed to approximate the unknown nonlinear functions in system dynamics due to their universal approximation capabilities. Particularly, NNs have been widely applied in various adaptive backstepping control methods [23]–[28]. As a matter of fact, the adaptation laws of these aforementioned methods were designed according to the stability of closed-loop systems alone. However, the original intent of using NNs for approximation was ignored [29]. And the performances of NNs for identifying unknown model dynamics were not seriously considered in most of the existing adaptive neural backstepping control methods [30]–[32]. In practice, the approximation precision of NNs has a major impact on the closed-loop control systems, which motivates us to improve the accuracy of the NN-based identified model. Fortunately, the approximation performances of NNs can be evaluated by constructing prediction errors obtained from serial–parallel estimation models. Hence, the prediction errors can be used to enhance the approximation precision of NNs. Inspired by the idea, some interesting works concerning composite adaptive neural control were presented by using the combination of tracking errors and prediction errors for weight adaptation [3], [29], [33], [34]. Similarly, composite adaptive fuzzy backstepping control was also reported in [35] and [36] by utilizing the information of prediction errors. Although many contributions have been made in the aforesaid excellent works, these methods can only guarantee infinite-time stability, which implies that the errors in their closed-loop systems can be convergent only when the time approaches infinity.

Different from asymptotic control methods, the finite-time control technique ensures that the desired system performance can be realized in finite time. Besides, the finite-time control technique brings the closed-loop system better robustness [37]–[39]. Because of the above advantages, the finite-time control technique has become more desirable and attracted considerable interest in recent years [40]. Hence, the exploration of finite-time command-filtered composite adaptive control is of great significance. Many finite-time control

Manuscript received March 23, 2020; revised July 28, 2020; accepted October 2, 2020. This work was supported in part by the National Natural Science Foundation of China under Grant 61421004, and in part by the National Science Foundation under Grant ECCS 1917275. This article was recommended by Associate Editor M. Forti.

Jinlin Sun, Jianqiang Yi, and Zhiqiang Pu are with the Institute of Automation, Chinese Academy of Sciences, Beijing 100190, China, and also with the School of Artificial Intelligence, University of Chinese Academy of Sciences, Beijing 100049, China (e-mail: jinlinsun@outlook.com; jianqiang.yi@ia.ac.cn; zhiqiang.pu@ia.ac.cn).

Haibo He is with the Department of Electrical, Computer and Biomedical Engineering, University of Rhode Island, Kingston, RI 02881 USA (e-mail: haibohe@uri.edu).

Color versions of one or more of the figures in this article are available online at https://ieeexplore.ieee.org.

Digital Object Identifier 10.1109/TCYB.2020.3032096

methods were presented for various nonlinear systems, including constrained systems [41]; multiagent systems [42], [43]; and switching systems [44]. Yu *et al.* [45] designed a pioneering finite-time command-filtered backstepping control scheme for nonlinear systems with strong robustness. However, the concerned system model was assumed to be known and no uncertainties were considered in this article. To deal with unknown nonlinearities, some finite-time convergent adaptive control methods were developed, including finite-time adaptive neural control [46]–[48] and finite-time adaptive fuzzy control [49], [50]. Sun *et al.* [47] designed a finite-time adaptive neural tracking control scheme for nonlinear systems in nonstrict feedback form. Lately, Li [51] developed a finite-time adaptive command-filtered backstepping control scheme with fault tolerance for strict-feedback uncertain nonlinear systems. Despite many superiorities, there still exist two issues to be further addressed. First, the designed parameter adaptation laws were driven by only tracking errors, which were not able to guarantee precise approximations. Second, the proposed control scheme was not able to deal with time-varying external disturbances that are commonly seen in engineering practice.

To the best of our knowledge, the problem of finite-time command-filtered composite adaptive control design for higher-order nonlinear systems in the presence of unknown nonlinearities, parameter uncertainties, and external disturbances is still open and remains unsolved. Motivated by the above observations, we propose a finite-time convergent command-filtered composite adaptive neural control scheme for the first time, featuring rapid response, strong robustness, and high-tracking accuracy. First, radial basis function NNs (RBFNNs) are utilized to approximate the unknown nonlinear functions of the considered system. Then, to improve the approximation precision of the RBFNNs, some novel composite adaptation laws driven by tracking errors and prediction errors are designed for updating weights. In addition, some new adaptive neural disturbance observers (ANDOs) are designed to estimate and compensate disturbances. Finally, based on the composite adaptive RBFNNs and the ANDOs, the nonsmooth command-filtered composite adaptive neural control scheme is developed to achieve finite-time convergence of all signals in the closed-loop control system.

Compared with the existing results, the main contributions of this article are summarized as follows.

1) A finite-time convergent command-filtered composite adaptive neural control scheme is proposed for higher-order uncertain nonlinear systems for the first time in this article. Different from the virtual control laws design in existing backstepping approaches, a novel control law without singularity problem is designed at each step.
2) Unlike existing works for constructing prediction errors in composite adaptive control schemes, such as [3], [29], and [33]–[36], a new serial–parallel nonsmooth estimation model (SPNEM) is designed in this article, which further enhances the NN approximation precision.
3) Apart from external disturbances, the minimum approximation errors of NNs are estimated by designing ANDOs, which are different from conventional disturbance observers [52]. The performance and robustness of the control system can be greatly improved by utilizing the ANDOs for disturbance compensation.
4) The nonsmooth command filters introduced in this article can converge faster than the existing linear filters in [11] and [51]. In addition, the parameters of the nonsmooth command filters are easier to tune, as compared to those of the differentiators in [45].

The remainder of this article is organized as follows. Section II addresses the problem formulation. Section III gives the control scheme design procedure and the closed-loop stability analysis. Simulations of two representative examples are conducted in Section IV to verify the effectiveness of the proposed control scheme. Finally, Section V concludes this article.

II. Problem Formulation

Consider the tracking control problem of the following class of the nth-order uncertain nonlinear system:

$$\begin{cases} \dot{x}_i = f_i(\bar{x}_i) + g_i(\bar{x}_i)x_{i+1} + d_i, \ \ i = 1, 2, \dots, n-1 \\ \dot{x}_n = f_n(\bar{x}_n) + g_n(\bar{x}_n)u + d_n \\ y = \ x_1 \end{cases} \tag{1}$$

where $\bar{x}_i = [x_1, x_2, \dots, x_i]^T \in \mathbb{R}^i$, $\bar{x}_n = [x_1, x_2, \dots, x_n]^T \in \mathbb{R}^n$ is the system state vector, $u \in \mathbb{R}$ is the control input, and $y \in \mathbb{R}$ is the output variable. Besides, $f_i(\bar{x}_i) \in \mathbb{R}$, $g_i(\bar{x}_i) \in \mathbb{R}$, and $d_i \in \mathbb{R}$ denote the unknown nonlinearities, the nominal control-gain functions, and the time-varying external disturbances, respectively. The control objective is to design a composite adaptive neural control scheme such that the output y tracks the reference signal y_d in finite time, where y_d and its time derivative up to second order are known and bounded.

Assumption 1 [1] and [11]: There exist positive constants ϑ_{0i}, ϑ_{1i} $(i = 1, 2, \dots, n)$ such that the external disturbances d_i satisfy $|d_i| \leq \vartheta_{0i}$ and $|\dot{d}_i| \leq \vartheta_{1i}$.

Assumption 2 [45]: There exist positive constants η_i such that $|g_i(\bar{x}_i)| \leq \eta_i$, $i = 1, 2, \dots, n$.

Taking the parameter uncertainties in the system dynamics into account, the uncertain nonlinear system (1) is derived as

$$\begin{cases} \dot{x}_i = \ F_i(\bar{x}_i) + g_i(\bar{x}_i)x_{i+1} + d_i, \ \ i = 1, 2, \dots, n-1 \\ \dot{x}_n = \ F_n(\bar{x}_n) + g_n(\bar{x}_n)u + d_n \\ y = \ x_1 \end{cases} \tag{2}$$

where $F_i(\bar{x}_i) = f_i(\bar{x}_i) + \Delta_i$, $F_n(\bar{x}_n) = f_n(\bar{x}_n) + \Delta_n$ are unknown functions. Besides, Δ_j, $j = 1, 2, \dots, n$, denote the lumped parameter uncertainties.

Remark 1: The nonlinear dynamics (2) considers unknown nonlinearities, parameter uncertainties, and time-varying external disturbances simultaneously. Hence, model (2) is more general than the models considered in [45] and [51].

Remark 2: The finite-time control in this article indicates that the desired system performance can be realized in finite time, which focuses on the convergence rate. Another concept of finite-time control in [53] means that the system state is no larger than a certain bound in the predefined finite-time span, which focuses on achieving superior transient performance. Note that the two concepts are different.

This article has been accepted for inclusion in a future issue of this journal. Content is final as presented, with the exception of pagination.

At the end of this section, some useful lemmas are listed below for the subsequent analyses.

Lemma 1 [54]: Consider the system $\dot{x} = f(x)$. Suppose there exist a continuous positive-definite Lyapunov function $V(x)$ and some real numbers $p_1 > 0$, $p_2 > 0$, and $0 < \alpha < 1$ such that $\dot{V}(x) \leq -p_1 V(x) - p_2 V^{\alpha}(x)$ holds, then the system $\dot{x} = f(x)$ is finite-time stable and the settling time can be given by

$$T \leq T_r := \frac{1}{p_1(1-\alpha)} \ln \frac{p_1 V^{1-\alpha}(x_0) + p_2}{p_2}. \tag{3}$$

Remark 3: The finite-time Lyapunov theorem in Lemma 1 was proposed by Yu *et al.* [54] with the form of the fast terminal sliding mode and has been widely used to prove the finite-time stability, such as [45] and [51]. Note that in some articles concerning finite-time control, the Lyapunov function condition $\dot{V}(x) \leq -p_2 V^{\alpha}(x)$ can also ensure finite-time stability. However, the proposed control scheme satisfying the Lyapunov function condition in Lemma 1 can ensure faster convergence [55].

Lemma 2 [56] and [57]: For any constant $0 < l < 1$, the following inequality holds for $\forall x_i \in \mathbb{R}, i = 1, \ldots, n$:

$$(|x_1| + |x_2| + \cdots + |x_n|)^l \leq |x_1|^l + |x_2|^l + \cdots + |x_n|^l. \tag{4}$$

Lemma 3 [57]: For any given positive constants p, q, and γ, the following inequality holds for $\forall x, y \in \mathbb{R}$:

$$|x|^p |y|^q \leq \frac{p}{p+q}\gamma |x|^{p+q} + \frac{q}{p+q}\gamma^{-\frac{p}{q}} |y|^{p+q}. \tag{5}$$

III. Control Scheme Design and Stability Analysis

In this section, we will propose a command-filtered composite adaptive neural control scheme with finite-time convergence for the uncertain nonlinear system (2). The detailed design procedure and stability analysis will be presented.

A. Brief Introduction of Neural Network

Given that the values of $F_i(\bar{x}_i)$, $i = 1, 2, \ldots, n$, in (2) are not available in practice, we use RBFNNs to identify these unknown nonlinear functions due to the universal approximation properties. The continuous function $F_i(\bar{x}_i){:}\Omega_{\bar{x}_i} \to \mathbb{R}$ over a compact set $\Omega_{\bar{x}_i} \subset \mathbb{R}^i$ can be approximated to arbitrary accuracy by an RBFNN as follows [26]:

$$F_i(\bar{x}_i) = W_i^{*T} S_i(\bar{x}_i) + \varepsilon_i \tag{6}$$

where $i = 1, 2, \ldots, n$, $W_i^* \in \mathbb{R}^{m_i}$ is the ideal constant weight vector, which is expressed as

$$W_i^* = \arg\min_{W_i \in \mathbb{R}^{m_i}} \left[\sup_{\bar{x}_i \in \Omega_{\bar{x}_i}} \left| F_i(\bar{x}_i) - W_i^T S_i(\bar{x}_i) \right| \right] \tag{7}$$

where W_i is the estimate of W_i^* and m_i denotes the number of hidden layer nodes of the RBFNN. The basic function vector $S_i(\bar{x}_i) = [s_{i1}(\bar{x}_i), \ldots, s_{im_i}(\bar{x}_i)]^T \in \mathbb{R}^{m_i}$ with $s_{ij}(\bar{x}_i)$ being selected as

$$s_{ij}(\bar{x}_i) = \exp\left[-\frac{(\bar{x}_i - \mu_{ij})^T (\bar{x}_i - \mu_{ij})}{\delta_i^2} \right] \tag{8}$$

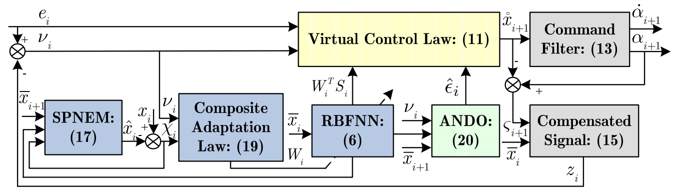

Fig. 1. Block diagram of the proposed control scheme (step i).

where $\mu_{ij} \in \mathbb{R}^i$ is the center of the receptive field and $\delta_i \in \mathbb{R}^+$ is the width of the Gaussian function. Besides, ε_i is the minimum function approximation error of the RBFNN satisfying $|\varepsilon_i| \leq \varepsilon_i^*$ with positive bounded constant ε_i^*. In the following, the function $S_i(\bar{x}_i)$ will be simplified as S_i for brevity. According to the definition of the basic function vector, $|S_i(\bar{x}_i)| \leq \sqrt{m_i}$ holds.

B. Finite-Time Command-Filtered Composite Adaptive Neural Controllers Design

In the following, the finite-time command-filtered composite adaptive control scheme design will be given step by step via a recursive approach. The virtual control laws will be designed in step i $(i = 1, 2, \ldots, n-1)$ and the actual control law will be designed in step n.

Step i $(i = 1, 2, \ldots, n-1)$: For clarity, the block diagram of the ith step of the proposed control scheme is presented in Fig. 1, which shows the design procedure. Defining $e_i = x_i - \alpha_i$ with $\alpha_1 = y_d$, $\tilde{W}_i = W_i^* - W_i$, and $\epsilon_i = \varepsilon_i + d_i$, we have

$$\dot{e}_i = W_i^T S_i + g_i(\bar{x}_i) x_{i+1} + \tilde{W}_i^T S_i + \epsilon_i - \dot{\alpha}_i. \tag{9}$$

Taking x_{i+1} as a virtual control input and following the idea in [45], the finite-time virtual control law $\check{x}_{i+1}$ is designed as

$$\check{x}_{i+1} = \frac{1}{g_i(\bar{x}_i)} \big[-k_{i1} e_i - k_{i2} \nu_i^{\gamma_i} - W_i^T S_i + \dot{\alpha}_i - g_{i-1}(\bar{x}_{i-1}) e_{i-1} \big] \tag{10}$$

with the constants $k_{i1}, k_{i2} > 0$, $0 < \gamma_i < 1$, where $\gamma_i = (p_i/q_i)$, p_i and q_i are positive odd integers satisfying $p_i < q_i$, and the variable ν_i denotes the compensated tracking error, which will be defined later. Besides, $g_0(\bar{x}_0) e_0 = 0$.

Actually, the nonlinear term $k_{i2}\nu_i^{\gamma_i}$ in (10) can accelerate the convergence rate of the compensated tracking error ν_i when $|\nu_i| \in (0, 1)$. However, its time derivative $k_{i2}\gamma_i \nu_i^{\gamma_i - 1}\dot{\nu}_i$ will lead to the singularity problem when $\nu_i = 0$ and $\dot{\nu}_i \neq 0$ due to $\gamma_i - 1 < 0$, which makes the command-filtered backstepping design lacks rigor.

To avoid this problem, we modify (10) and design a novel singularity-free virtual control law $\mathring{x}_{i+1}$ as

$$\mathring{x}_{i+1} = \frac{1}{g_i(\bar{x}_i)} \big[-k_{i1} e_i - k_{i2} \varphi_i(\nu_i) - W_i^T S_i + \dot{\alpha}_i - g_{i-1}(\bar{x}_{i-1}) e_{i-1} - \hat{\epsilon}_i \big] \tag{11}$$

with the nonlinear function $\varphi_i(\nu_i)$ designed as

$$\varphi_i(\nu_i) = \begin{cases} \lceil \nu_i \rfloor^{\varrho}, & \text{if } |\nu_i| \geq \xi_i \\ c_{i1}\nu_i + c_{i2}\nu_i^3, & \text{if } |\nu_i| < \xi_i \end{cases} \tag{12}$$

where the constants $0 < \varrho < 1$ and $0 < \xi_i \leq 1$. The notation $\lceil x \rfloor^{\varrho} = |x|^{\varrho}\text{sign}(x)$ is introduced in this article to simplify expression. Besides, $c_{i1} = ((3-\varrho)/2)\xi_i^{\varrho-1}$ and $c_{i2} = ((\varrho - 1)/2)\xi_i^{\varrho-3}$. These parameters are chosen to satisfy $c_{i1} + c_{i2} \geq 0$. In addition, $\hat{\epsilon}_i$ is the estimation of ϵ_i by using an ANDO, which will be designed in (20).

Remark 4: Note that the singularity problem will not occur through using the virtual control law (11) in the command-filtered backstepping design procedure. Specifying the coefficients c_{i1} and c_{i2}, we can ensure that the nonlinear function $\varphi_i(\nu_i)$ and its time derivative are both continuous. Besides, in (10), the term $\nu_i^{\gamma_i} \notin \mathbb{R}$ when $x < 0$. In contrast, the control law (11) circumvents this problem by designing $\varphi_i(\nu_i)$.

Note that the function $\varphi_i(\nu_i)$ can be divided into a nonsmooth term and a smooth term. In fact, similar to $\nu_i^{\gamma_i}$ in (10), the nonsmooth term $\lceil \nu_i \rfloor^{\varrho}$ in $\varphi_i(\nu_i)$ can also accelerate the convergence rate of ν_i when $|\nu_i| \in (0, 1)$. Generally, one can select a small enough ξ_i to guarantee that the nonsmooth term $\lceil \nu_i \rfloor^{\varrho}$ dominates $\varphi_i(\nu_i)$ during the entire control process.

To avoid repeated analytic differentiation of virtual control laws, we introduce a new nonsmooth command filter as

$$\begin{aligned} \tau_{i+1}\dot{\alpha}_{i+1} &= \lceil \mathring{x}_{i+1} - \alpha_{i+1} \rfloor^{\varrho} + (\mathring{x}_{i+1} - \alpha_{i+1}) \\ \alpha_{i+1}(0) &= \mathring{x}_{i+1}(0) \end{aligned} \tag{13}$$

where the filter parameter τ_{i+1} is a positive constant.

Remark 5: The command filter is a prefilter by treating virtual control law as the input and it generates the filtered virtual control law and the derivative of the virtual control law. In practice, command filters are introduced to avoid computing analytic derivatives and eliminate the problem of the explosion of complexity in traditional backstepping approaches [8].

Remark 6: Compared with existing methods, the command filter (13) has some advantages. First, the nonsmooth command filter is finite-time convergent, which can converge faster than the linear filter used in [11] and [51]. Second, the parameters of the nonsmooth command filter are easier to tune than those of the widely used Levant differentiator in [45].

Define $e_{i+1} = x_{i+1} - \alpha_{i+1}$ and $\varsigma_{i+1} = \alpha_{i+1} - \mathring{x}_{i+1}$. Then, the derivative of e_i is given as

$$\begin{aligned} \dot{e}_i = &-k_{i1}e_i - k_{i2}\varphi_i(\nu_i) + \tilde{W}_i^T S_i + \tilde{\epsilon}_i + g_i(\bar{x}_i)e_{i+1} \\ &+ g_i(\bar{x}_i)\varsigma_{i+1} - g_{i-1}(\bar{x}_{i-1})e_{i-1}. \end{aligned} \tag{14}$$

In order to remove the effect of the filtering error ς_{i+1}, the compensating signal z_i is designed as

$$\begin{aligned} \dot{z}_i = &-k_{i1}z_i + g_i(\bar{x}_i)(z_{i+1} + \varsigma_{i+1}) \\ &- g_{i-1}(\bar{x}_{i-1})z_{i-1} - l_i\text{sign}(z_i), \;\; z_i(0) = 0 \end{aligned} \tag{15}$$

where the constant $l_i > 0$ and $g_0(\bar{x}_0)z_0 = 0$. z_{i+1} will be defined in the next step. Defining the compensated tracking error $\nu_i = e_i - z_i$ yields

$$\begin{aligned} \dot{\nu}_i = &-k_{i1}\nu_i - k_{i2}\varphi_i(\nu_i) + \tilde{W}_i^T S_i + g_i(\bar{x}_i)\nu_{i+1} \\ &- g_{i-1}(\bar{x}_{i-1})\nu_{i-1} + l_i\text{sign}(z_i) + \tilde{\epsilon}_i. \end{aligned} \tag{16}$$

To enhance the approximation performance of the RBFNN $W_i^T S_i$, a composite adaptation law will be designed for weights updating. Defining the prediction error as $\chi_i = x_i - \hat{x}_i$, where $\hat{x}_i$ is obtained from the following SPNEM:

$$\dot{\hat{x}}_i = W_i^T S_i + g_i(\bar{x}_i)x_{i+1} + \kappa_{i1}\chi_i + \kappa_{i2}\lceil \chi_i \rfloor^{\varrho} \tag{17}$$

we obtain

$$\dot{\chi}_i = \tilde{W}_i^T S_i - \kappa_{i1}\chi_i - \kappa_{i2}\lceil \chi_i \rfloor^{\varrho} + \epsilon_i. \tag{18}$$

Remark 7: As a matter of fact, the actual approximation error of $W_i^T S_i$ cannot be obtained directly because $F_i(\bar{x}_i)$ is unknown. Fortunately, the approximation error of $W_i^T S_i$ can be reflected by constructing the SPNEM (17) to generate the prediction error χ_i. In addition, different from the linear-feedback methods for constructing prediction errors in the existing composite adaptive control [3], [29], [33]–[36], the designed SPNEM contains the fractional power term $\lceil \chi_i \rfloor^{\varrho} = |\chi_i|^{\varrho}\text{sign}(\chi_i)$. On the one hand, this term contributes to the finite-time convergence of the closed-loop control system. By designing the SPNEM, we can obtain the dynamics of the prediction error as (18), which lays a foundation for the finite-time convergence analysis of the closed-loop system. On the other hand, the fractional power term is conductive to achieving better approximation precision of the ith RBFNN and overall tracking performances.

Then, the predictor error χ_i and the compensated tracking error ν_i are employed to construct the composite adaptation law of W_i with σ-modification, which is given as

$$\dot{W}_i = \beta_i(\nu_i + \beta_{i1}\chi_i)S_i - \sigma_i W_i \tag{19}$$

where β_i, β_{i1}, and σ_i are positive constants.

Remark 8: The prediction error χ_i reflects the approximation error of the RBFNN $W_i^T S_i$. Hence, the approximation precision of $W_i^T S_i$ is improved by using the feedback of the prediction error and the tracking error simultaneously to design the composite adaptation law (19), which is different from the existing adaptation laws [30]–[32], [46], [49]–[51]. In contrast, the conventional adaptation laws are designed according to the stability of closed-loop systems alone and the performance of NNs for identifying unknown models is not seriously considered. Hence, the composite adaptation law (19) is superior to the conventional adaptation laws in that the composite adaptation law can enhance the approximation precision of NNs and improve the closed-loop tracking performance consequently.

Usually, external disturbances can be estimated by using model-based disturbance observers [52]. Here, the external disturbance and the minimum approximation error of the ith RBFNN are integrated as ϵ_i. The ith ANDO for estimating the lumped disturbance ϵ_i is designed by using NN approximation

$$\begin{cases} \dot{h}_i = -\lambda_i(h_i + \lambda_i x_i) - \lambda_i(W_i^T S_i + g_i(\bar{x}_i)x_{i+1}) + \nu_i \\ \hat{\epsilon}_i = \;\; h_i + \lambda_i x_i \end{cases} \tag{20}$$

where h_i is an internal state and λ_i is a positive constant.

Remark 9: In this article, the ANDO is designed to estimate and compensate for the lumped disturbance. Alternatively, if the considered system suffers from multiple disturbances, and the disturbances can be divided into different parts, the composite anti-disturbance control [58] can be used.

Defining $\tilde{\epsilon}_i = \epsilon_i - \hat{\epsilon}_i$, we obtain

$$\dot{\tilde{\epsilon}}_i = -\lambda_i\tilde{\epsilon}_i - \lambda_i\tilde{W}_i^T S_i + \dot{\epsilon}_i - \nu_i. \quad (21)$$

Step n: Defining $e_n = x_n - \alpha_n$, $\tilde{W}_n = W_n^* - W_n$, and $\epsilon_n = \varepsilon_n + d_n$, we can write the dynamics of e_n as

$$\dot{e}_n = W_n^T S_n + g_n(\bar{x}_n)u + \tilde{W}_n^T S_n + \epsilon_n - \dot{\alpha}_n. \quad (22)$$

The finite-time actual control law u is designed as

$$u = \frac{1}{g_n(\bar{x}_n)}\left[-k_{n1}e_n - k_{n2}\varphi_n(\nu_n) - W_n^T S_n + \dot{\alpha}_n - g_{n-1}(\bar{x}_{n-1})e_{n-1} - \hat{\epsilon}_n\right] \quad (23)$$

with the constants $k_{n1}, k_{n2} > 0$, and the variable ν_n denotes the compensated tracking error, which will be defined later. Besides, $\hat{\epsilon}_n$ is the estimation of ϵ_n by using an ANDO, which will be designed in (31). The function $\varphi_n(\nu_n)$ is designed as

$$\varphi_n(\nu_n) = \begin{cases} \lceil \nu_n \rfloor^{\varrho}, & \text{if } |\nu_n| \geq \xi_n \\ c_{n1}\nu_n + c_{n2}\nu_n^3, & \text{if } |\nu_n| < \xi_n \end{cases} \quad (24)$$

where the constants $0 < \xi_n \leq 1$, $c_{n1} = ((3-\varrho)/2)\xi_n^{\varrho-1}$, and $c_{n2} = ((\varrho-1)/2)\xi_n^{\varrho-3}$. The parameters are chosen to satisfy $c_{n1} + c_{n2} \geq 0$.

Then, the derivative of e_n is given as

$$\dot{e}_n = -k_{n1}e_n - k_{n2}\varphi_n(\nu_n) + \tilde{W}_n^T S_n - g_{n-1}(\bar{x}_{n-1})e_{n-1} + \tilde{\epsilon}_n. \quad (25)$$

The compensating signal z_n is designed as

$$\dot{z}_n = -k_{n1}z_n - g_{n-1}(\bar{x}_{n-1})z_{n-1} - l_n\text{sign}(z_n),\ z_n(0) = 0 \quad (26)$$

where the constant $l_n > 0$. Then, defining the compensated tracking error as $\nu_n = e_n - z_n$, we have

$$\dot{\nu}_n = -k_{n1}\nu_n - k_{n2}\varphi_n(\nu_n) + \tilde{W}_n^T S_n - g_{n-1}(\bar{x}_{n-1})\nu_{n-1} + l_n\text{sign}(z_n) + \tilde{\epsilon}_n. \quad (27)$$

To enhance the approximation performance of the RBFNN $W_n^T S_n$, a composite adaptation law will be designed for weights updating. Defining the prediction error as $\chi_n = x_n - \hat{x}_n$, where $\hat{x}_n$ is obtained from the SPNEM

$$\dot{\hat{x}}_n = W_n^T S_n + g_n(\bar{x}_n)u + \kappa_{n1}\chi_n + \kappa_{n2}\lceil \chi_n \rfloor^{\varrho} \quad (28)$$

we can obtain

$$\dot{\chi}_n = \tilde{W}_n^T S_n - \kappa_{n1}\chi_n - \kappa_{n2}\lceil \chi_n \rfloor^{\varrho} + \epsilon_n. \quad (29)$$

Then, the predictor error χ_n and the compensated tracking error ν_n are employed to construct the composite adaptation law of W_n with σ-modification, which is given as

$$\dot{W}_n = \beta_n(\nu_n + \beta_{n1}\chi_n)S_n - \sigma_n W_n \quad (30)$$

where β_n, β_{n1}, and σ_n are positive constants.

The nth ANDO for estimating the lumped disturbance ϵ_n is designed by using RBFNN approximation, shown as

$$\begin{cases} \dot{h}_n = -\lambda_n(h_n + \lambda_n x_n) - \lambda_n(W_n^T S_n + g_n(\bar{x}_n)u) + \nu_n \\ \hat{\epsilon}_n = h_n + \lambda_n x_n \end{cases} \quad (31)$$

where h_n is an internal state and λ_n is a positive constant.

Defining $\tilde{\epsilon}_n = \epsilon_n - \hat{\epsilon}_n$, we have

$$\dot{\tilde{\epsilon}}_n = -\lambda_n\tilde{\epsilon}_n - \lambda_n\tilde{W}_n^T S_n + \dot{\epsilon}_n - \nu_n. \quad (32)$$

Remark 10: Compared to previous works, some new difficulties appear in our control scheme design process. First, to obtain the finite-time virtual control laws in the command-filtered backstepping framework, one may come across the singularity problem, as shown in (10), by following the previous works. And it is challenging to design finite-time virtual control laws to circumvent the singularity problem. Second, most of the existing results concerning composite adaptive backstepping control can only achieve infinite-time convergence. In fact, it is challenging to realize the finite-time convergence of all signals in the closed-loop control system, including the tracking errors, prediction errors, parameter estimation errors of RBFNNs, and lumped disturbance estimation errors. Third, it is difficult to design a finite-time command filter which can converge faster than the previous filters and is featured with less parameters.

C. Stability Analysis

Now, we are ready to give the closed-loop stability analysis of the proposed control system.

Theorem 1: Consider the closed-loop system consisting of the uncertain nonlinear plant (2), the virtual control laws (11), the actual control law (23), the composite adaptation laws (19), (30), the ANDOs (20), (31), and the command filters (13) under Assumptions 1 and 2. Then, the tracking error $e_1 = y - y_d$ converges to an arbitrary small neighborhood around zero in finite time by choosing suitable parameters and all signals in the closed-loop system are bounded in finite time.

Proof: Consider the Lyapunov function candidate as

$$V = \frac{1}{2}\left(\sum_{i=1}^n \nu_i^2 + \sum_{i=1}^n \beta_{i1}\chi_i^2 + \sum_{i=1}^n \frac{1}{\beta_i}\tilde{W}_i^T\tilde{W}_i + \sum_{i=1}^n \tilde{\epsilon}_i^2\right). \quad (33)$$

Differentiating (33) with respect to time obtains

$$\begin{aligned}\dot{V} &= \sum_{i=1}^n \nu_i\dot{\nu}_i + \sum_{i=1}^n \beta_{i1}\chi_i\dot{\chi}_i - \sum_{i=1}^n \frac{1}{\beta_i}\tilde{W}_i^T\dot{W}_i + \sum_{i=1}^n \tilde{\epsilon}_i\dot{\tilde{\epsilon}}_i \\ &\leq \sum_{i=1}^n\Big(-k_{i1}\nu_i^2 - k_{i2}\nu_i\varphi_i(\nu_i) - \kappa_{i1}\beta_{i1}\chi_i^2 \\ &\quad - \kappa_{i2}\beta_{i1}|\chi_i|^{\varrho+1} - \lambda_i\tilde{\epsilon}_i^2\Big) + \sum_{i=1}^n\Big(\beta_{i1}|\chi_i||\epsilon_i| \\ &\quad + \frac{\sigma_i}{\beta_i}\tilde{W}_i^T W_i + \lambda_i|\tilde{\epsilon}_i||\tilde{W}_i^T S_i| + |\tilde{\epsilon}_i||\dot{\epsilon}_i| + l_i|\nu_i\text{sign}(z_i)|\Big). \end{aligned} \quad (34)$$

The next part is divided into three cases.

Case 1: When all ν_i satisfy $|\nu_i| \geq \xi_i$, $i = 1, \ldots, n$, using Lemma 2, we obtain that

$$\begin{aligned}\sum_{i=1}^n -k_{i2}\nu_i\varphi_i(\nu_i) &= \sum_{i=1}^n -2^{\alpha}k_{i2}\left(\frac{1}{2}\nu_i^2\right)^{\alpha} \\ &\leq -r_1\left(\sum_{i=1}^n \frac{1}{2}\nu_i^2\right)^{\alpha} \end{aligned} \quad (35)$$

where $r_1 = \min\{2^{((\varrho+1)/2)}k_{12}, \ldots, 2^{((\varrho+1)/2)}k_{n2}\}$ and $\alpha = ((\varrho+1)/2)$.

Case 2: When there are only m $(1 \leq m < n)$ compensated tracking errors satisfying $|\nu_i| \geq \xi_i$, we have

$$\sum_{i=1}^{n} -k_{i2}\nu_i\varphi_i(\nu_i) = \sum_{j=1}^{m} -\overline{k}_{j2}|\overline{\nu}_j|^{\varrho+1} + \sum_{j=1}^{n-m} -\underline{k}_{j2}(\underline{c}_{j1}\underline{\nu}_j^2 + \underline{c}_{j2}\underline{\nu}_j^4). \quad (36)$$

In (36), when $|\nu_i| \geq \xi_i$ $(1 \leq i \leq n)$, we rewrite ν_i as $\overline{\nu}_j$ $(1 \leq j \leq m)$ and rewrite k_{i2} as $\overline{k}_{j2}$. When $|\nu_i| < \xi_i$ $(1 \leq i \leq n)$, we rewrite ν_i, k_{i2}, c_{i1}, and c_{i2} as $\underline{\nu}_j$, $\underline{k}_{j2}$, $\underline{c}_{j1}$, and $\underline{c}_{j2}$ $(1 \leq j \leq n-m)$, respectively. Given that $\underline{k}_{j2} > 0$, $\underline{c}_{j2} < 0$, $|\underline{\nu}_j| < \xi_i \leq 1$, it is obtained that $-\underline{k}_{j2}\underline{c}_{j2}\underline{\nu}_j^4 \leq -\underline{k}_{j2}\underline{c}_{j2}\underline{\nu}_j^2$. Then, using Lemma 2, we have

$$\sum_{i=1}^{n} -k_{i2}\nu_i\varphi_i(\nu_i) \leq -r_2\left(\sum_{j=1}^{m}\frac{1}{2}\overline{\nu}_j^2\right)^{\alpha} - r_2\left(\sum_{j=m+1}^{n}\frac{1}{2}\overline{\nu}_j^2\right)^{\alpha} + r_2\left(\sum_{j=m+1}^{n}\frac{1}{2}\overline{\nu}_j^2\right)^{\alpha} + \sum_{j=1}^{n-m} -\underline{k}_{j2}(\underline{c}_{j1} + \underline{c}_{j2})\underline{\nu}_j^2 \quad (37)$$

where $r_2 = \min\{2^{\alpha}\overline{k}_{12}, \ldots, 2^{\alpha}\overline{k}_{m2}\}$, $\overline{\nu}_j$ $(m+1 \leq j \leq n)$ denotes the compensated tracking error that satisfies $|\overline{\nu}_j| < \xi_i$.

Applying Lemma 2 to (37) and using Lemma 3 with $p = 1-\alpha$, $q = \alpha$, $\gamma = \alpha^{(\alpha/(1-\alpha))}$, $x = 1$, and $y = \sum_{j=m+1}^{n}(1/2)\overline{\nu}_j^2$, we obtain

$$\sum_{i=1}^{n} - k_{i2}\nu_i\varphi_i(\nu_i) \leq -r_2\left(\sum_{j=1}^{n}\frac{1}{2}\overline{\nu}_j^2\right)^{\alpha} + r_2(1-\alpha)\alpha^{\frac{\alpha}{1-\alpha}} + r_2\sum_{j=m+1}^{n}\frac{1}{2}\overline{\nu}_j^2 + \sum_{j=1}^{n-m} -\underline{k}_{j2}(\underline{c}_{j1} + \underline{c}_{j2})\underline{\nu}_j^2. \quad (38)$$

Case 3: When all ν_i satisfy $|\nu_i| < \xi_i$, $i = 1, \ldots, n$, following the similar steps in case 2, we have

$$\sum_{i=1}^{n} - k_{i2}\nu_i\varphi_i(\nu_i) \leq -r_2\left(\sum_{i=1}^{n}\frac{1}{2}\nu_i^2\right)^{\alpha} + r_2(1-\alpha)\alpha^{\frac{\alpha}{1-\alpha}} + r_2\sum_{i=1}^{n}\frac{1}{2}\nu_i^2 + \sum_{i=1}^{n} -k_{i2}(c_{i1} + c_{i2})\nu_i^2. \quad (39)$$

Following the three cases, given that $r_1 \leq r_2$, $c_{i1} + c_{i2} \geq 0$, $i = 1, \ldots, n$, we can conclude that $\forall \nu_i \in \mathbb{R}$, the following inequality holds:

$$\sum_{i=1}^{n} -k_{i2}\nu_i\varphi_i(\nu_i) \leq - r_1\left(\sum_{i=1}^{n}\frac{1}{2}\nu_i^2\right)^{\alpha} + r_2(1-\alpha)\alpha^{\frac{\alpha}{1-\alpha}} + r_2\sum_{i=1}^{n}\frac{1}{2}\nu_i^2. \quad (40)$$

According to Young's inequality [2] and recalling the fact that $|S_i(\bar{x}_i)| \leq \sqrt{m_i}$, the following inequalities are obtained:

$$\frac{\sigma_i}{\beta_i}\tilde{W}_i^T W_i \leq -\frac{\sigma_i(2-\Lambda_i)}{2\beta_i}\tilde{W}_i^T\tilde{W}_i + \frac{\sigma_i}{2\beta_i\Lambda_i}\|W_i^*\|^2 \quad (41)$$

$$|\tilde{\epsilon}_i||\tilde{W}_i^T S_i| \leq \frac{1}{2}\tilde{\epsilon}_i^2 + \frac{m_i}{2}\|\tilde{W}_i\|^2 \quad (42)$$

$$|\chi_i||\epsilon_i| \leq \frac{1}{2}\chi_i^2 + \frac{1}{2}(\varepsilon_i^* + \vartheta_{0i})^2 \quad (43)$$

$$|\tilde{\epsilon}_i||\dot{\epsilon}_i| \leq \frac{1}{2}\tilde{\epsilon}_i^2 + \frac{1}{2}B_i^2 \quad (44)$$

$$l_i|\nu_i\mathrm{sign}(z_i)| \leq \frac{1}{2}\nu_i^2 + \frac{1}{2}l_i^2 \quad (45)$$

where $|\dot{\epsilon}_i| \leq B_i$, and B_i is a positive constant. $\Lambda_i \in (0, 1]$ is a positive constant to be determined.

Using the inequalities (40)–(45), one obtains

$$\begin{aligned}\dot{V} \leq& \sum_{i=1}^{n}\Bigg[-k_{i1}\nu_i^2 + \frac{r_2}{2}\nu_i^2 + \frac{1}{2}\nu_i^2 - \left(\kappa_{i1}\beta_{i1} - \frac{\beta_{i1}}{2}\right)\chi_i^2 \\ &-\left(\frac{\sigma_i(2-\Lambda_i)}{2\beta_i} - \frac{\lambda_i m_i}{2}\right)\tilde{W}_i^T\tilde{W}_i - \left(\frac{\lambda_i}{2} - \frac{1}{2}\right)\tilde{\epsilon}_i^2\Bigg] \\ &-r_1\left(\sum_{i=1}^{n}\frac{1}{2}\nu_i^2\right)^{\alpha} - \sum_{i=1}^{n}2^{\alpha}\kappa_{i2}\beta_{i1}^{1-\alpha}\left(\frac{\beta_{i1}}{2}\chi_i^2\right)^{\alpha} + \iota_1 \\ \leq& -r_3 V - r_4\sum_{i=1}^{n}\left[\left(\frac{1}{2}\nu_i^2\right)^{\alpha} + \left(\frac{\beta_{i1}}{2}\chi_i^2\right)^{\alpha}\right] + \iota_1 \end{aligned} \quad (46)$$

where $r_3 = \min\{(2k_{i1} - r_2 - 1), (2\kappa_{i1} - 1), (\sigma_i(2 - \Lambda_i) - \lambda_i\beta_i m_i), (\lambda_i - 1)\}$, $r_4 = \min\{r_1, 2^{\alpha}\kappa_{i2}\beta_{i1}^{1-\alpha}\}$ $(i = 1, 2, \ldots, n)$ are positive by choosing parameters and $\iota_1 = \sum_{i=1}^{n}[(\sigma_i/2\beta_i\Lambda_i)\|W_i^*\|^2 + (\beta_{i1}/2)(\varepsilon_i^* + \vartheta_{0i})^2 + (1/2)B_i^2 + r_2(1-\alpha)\alpha^{(\alpha/(1-\alpha))} + (1/2)l_i^2]$ is positive and bounded.

Following Lemma 2, we can obtain

$$\begin{aligned}\dot{V} \leq& -r_3 V - r_4\left[\sum_{i=1}^{n}\left(\frac{1}{2}\nu_i^2 + \frac{1}{2}\beta_{i1}\chi_i^2\right)\right]^{\alpha} \\ &-r_4\left[\sum_{i=1}^{n}\left(\frac{1}{2\beta_i}\tilde{W}_i^T\tilde{W}_i + \frac{1}{2}\tilde{\epsilon}_i^2\right)\right]^{\alpha} \\ &+r_4\left[\sum_{i=1}^{n}\left(\frac{1}{2\beta_i}\tilde{W}_i^T\tilde{W}_i + \frac{1}{2}\tilde{\epsilon}_i^2\right)\right]^{\alpha} + \iota_1. \end{aligned} \quad (47)$$

Applying Lemma 2 and using Lemma 3 with $p = 1 - \alpha$, $q = \alpha$, $\gamma = \alpha^{(\alpha/(1-\alpha))}$, $x = 1$, and $y = \sum_{i=1}^{n}((1/2\beta_i)\tilde{W}_i^T\tilde{W}_i + (1/2)\tilde{\epsilon}_i^2)$, we have

$$\begin{aligned}\dot{V} \leq& -r_3 V - r_4 V^{\alpha} \\ &+r_4\left[\sum_{i=1}^{n}\left(\frac{1}{2\beta_i}\tilde{W}_i^T\tilde{W}_i + \frac{1}{2}\tilde{\epsilon}_i^2\right)\right]^{\alpha} + \iota_1 \\ \leq& -r_3 V - r_4 V^{\alpha} + r_4\Bigg[(1-\alpha)\alpha^{\frac{\alpha}{1-\alpha}} \\ &+\sum_{i=1}^{n}\left(\frac{1}{2\beta_i}\tilde{W}_i^T\tilde{W}_i + \frac{1}{2}\tilde{\epsilon}_i^2\right)\Bigg] + \iota_1 \\ \leq& -r_5 V - r_4 V^{\alpha} + \iota_2 \end{aligned} \quad (48)$$

where $r_5 = r_3 - r_4$ is chosen to be positive. $\iota_2 = \iota_1 + r_4(1-\alpha)\alpha^{(\alpha/(1-\alpha))}$ is positive and bounded.

According to (48), we obtain $\dot{V} \leq -r_5 V + \iota_2$. Solving it, we can obtain the following inequality: $V(t) \leq (\iota_2/r_5) + (V(0) - (\iota_2/r_5))e^{-r_5 t}$. Consequently, all signals of the closed-loop control system are uniformly ultimately bounded.

Next, in order to relax the conservatism, the subsequent proof procedure will be divided into two cases. First, define the error vector of the closed-loop control system as $\Xi = [\nu_i, \chi_i, \tilde{W}_i, \tilde{\epsilon}_i]^T$ $(i = 1, 2, \ldots, n)$ and define $\Omega_1 = \{\Xi | V \le (\iota_2/\zeta r_5)\}$ for any $0 < \zeta < 1$. Besides, Ω_2 is defined as the complement set of Ω_1. When Ξ is outside of Ω_1, that is, $\Xi \in \Omega_2$ and $V > (\iota_2/\zeta r_5)$, the inequality (48) can be rewritten as

$$\begin{aligned}\dot{V} &\le -\zeta r_5 V - (1-\zeta) r_5 V - r_4 V^{\alpha} + \iota_2 \\ &\le -(1-\zeta) r_5 V - r_4 V^{\alpha}\end{aligned} \tag{49}$$

where $(1-\zeta)r_5 > 0$, $r_4 > 0$, and $0 < \alpha < 1$. According to Lemma 1, the error vector Ξ will converge to Ω_1 in finite time and the settling time is estimated by

$$T_{r1} \le \frac{1}{r_5(1-\zeta)(1-\alpha)} \ln \frac{(1-\zeta) r_5 V^{1-\alpha}(0) + r_4}{r_4}. \tag{50}$$

Second, define $\Omega_3 = \{\Xi | V \le (\iota_2/\zeta r_4)^{(1/\alpha)}\}$. Besides, Ω_4 is defined as the complement set of Ω_3. When Ξ is outside of Ω_3, that is, $\Xi \in \Omega_4$ and $V > (\iota_2/\zeta r_4)^{(1/\alpha)}$, we have

$$\begin{aligned}\dot{V} &\le -r_5 V - \zeta r_4 V^{\alpha} - (1-\zeta) r_4 V^{\alpha} + \iota_2 \\ &\le -r_5 V - (1-\zeta) r_4 V^{\alpha}\end{aligned} \tag{51}$$

where $r_5 > 0$, $(1-\zeta)r_4 > 0$. According to Lemma 1, the error vector Ξ will converge to Ω_3 in finite time and the settling time is estimated by

$$T_{r2} \le \frac{1}{r_5(1-\alpha)} \ln \frac{r_5 V^{1-\alpha}(0) + (1-\zeta) r_4}{(1-\zeta) r_4}. \tag{52}$$

To summarize, the error vector Ξ will converge to a small region around the origin, that is, $\{\Xi | V \le \min\{(\iota_2/\zeta r_5), (\iota_2/\zeta r_4)^{(1/\alpha)}\}\}$, in finite time $T_1 = \max\{T_{r1}, T_{r2}\}$. Then, we obtain $(1/2)\nu_i^2 \le V \le \min\{(\iota_2/\zeta r_5), (\iota_2/\zeta r_4)^{(1/\alpha)}\}$ when $t \ge T_1$. Furthermore, ν_i will converge to the region $|\nu_i| \le \min\{\sqrt{(2\iota_2/\zeta r_5)}, \sqrt{2(\iota_2/\zeta r_4)^{(1/\alpha)}}\}$ when $t \ge T_1$. Namely, the compensated tracking error $\nu_1 = e_1 - z_1$ will converge to an arbitrary small neighborhood around zero in finite time T_1 by adjusting the design parameters.

In the following, it will be shown that the compensating signals $z_1, z_2, \ldots, z_n$ converge to zero in finite time. Generally, the process is divided into two steps. The first step is to analyze the boundedness of the filtering errors ς_i and the second step is to prove the convergence of the compensating signals z_i. First, construct a Lyapunov function candidate as

$$V_1 = \sum_{i=2}^{n} \frac{1}{2} \varsigma_i^2. \tag{53}$$

Then, the time derivative of V_1 is shown as

$$\dot{V}_1 = \left(\sum_{i=2}^{n} -\frac{1}{\tau_i} \varsigma_i^2 - \frac{1}{\tau_i} |\varsigma_i|^{\varrho+1} - \varsigma_i \frac{d}{dt} \mathring{x}_i \right) \tag{54}$$

where $(1/\tau_i) > 0$. Given that all signals in the closed-loop control system are bounded, the derivative of $\mathring{x}_i$ is bounded. Namely, $|(d/dt)\mathring{x}_i| \le L$ holds, where L is a positive constant. Then

$$\dot{V}_1 \le -r_6 V_1 - r_7 V_1^{\alpha} + \frac{1}{2} L^2 \tag{55}$$

where $r_6 = \min\{(2/\tau_2) - 1, (2/\tau_3) - 1, \ldots, (2/\tau_n) - 1\} > 0$, $r_7 = \min\{(2^{\alpha}/\tau_2), (2^{\alpha}/\tau_3), \ldots, (2^{\alpha}/\tau_n)\} > 0$, and $(1/2)L^2$ is a positive constant. Similar to the previous analyses, we obtain that $|\varsigma_i| \le \rho_{i-1}$ can be achieved in finite time, where $\rho_{i-1} = \sqrt{(L^2/\zeta r_6)}$ is positive and bounded. In addition, the settling time can be estimated by

$$T_0 \le \frac{1}{r_6(1-\zeta)(1-\alpha)} \ln \frac{(1-\zeta) r_6 V_1^{1-\alpha}(0) + r_7}{r_7}. \tag{56}$$

Second, choose a Lyapunov function candidate as

$$V_2 = \sum_{i=1}^{n} \frac{1}{2} z_i^2. \tag{57}$$

Differentiating V_2 with respect to time obtains

$$\dot{V}_2 = \sum_{i=1}^{n} \left(-k_{i1} z_i^2 \right) + \sum_{i=1}^{n} (-l_i |z_i|) + \sum_{i=1}^{n-1} g_i z_i \varsigma_{i+1}. \tag{58}$$

For $t \ge T_0$ and from Assumption 2, we have

$$\begin{aligned}\dot{V}_2 &= -\sum_{i=1}^{n} k_{i1} z_i^2 - \sum_{i=1}^{n} l_i |z_i| + \sum_{i=1}^{n-1} \eta_i \rho_i |z_i| + \eta_n \rho_n |z_n| \\ &\le -r_8 V_2 - r_9 V_2^{\frac{1}{2}}\end{aligned} \tag{59}$$

where $r_8 = \min\{2k_{i1}\}$, $r_9 = \min\{\sqrt{2}(l_i - \eta_i \rho_i)\}$ $(i = 1, 2, \ldots, n)$, and ρ_n is a positive constant. According to Lemma 1, by choosing suitable parameters such that $l_i > \eta_i \rho_i$ holds, the compensating signals $z_1, z_2, \ldots, z_n$ will converge to zero in finite time and the settling time is estimated by

$$T_2 \le T_0 + \frac{2}{r_8} \ln \frac{r_8 V_2^{\frac{1}{2}}(0) + r_9}{r_9}. \tag{60}$$

Recalling that $e_i = \nu_i + z_i$, the tracking errors will all converge to the region $|e_i| \le \min\{\sqrt{(2\iota_2/\zeta r_5)}, \sqrt{2(\iota_2/\zeta r_4)^{(1/\alpha)}}\}$ in finite time and the settling time is bounded by $T \le \max\{T_1, T_2\}$. Hence, e_1 will converge to an arbitrary small neighborhood around zero in finite time by adjusting the design parameters. This completes the proof. ■

Remark 11: In comparison with existing works, the novelties of the proposed command-filtered composite adaptive backstepping control scheme are three-fold. First, a new nonsmooth command filter is introduced in the control scheme, which can converge faster than the linear filter used in [11] and [51]. Besides, the parameters of the nonsmooth command filter are easier to tune than those of the widely used Levant differentiator in [45]. Second, the approximation precision of RBFNNs is improved by using the feedback of the prediction error and the tracking error simultaneously to design the composite adaptation law of the control scheme, which is different from the existing adaptation laws [30]–[32]. In addition, different from the linear-feedback methods for constructing prediction errors in the existing composite adaptive control [3], [33]–[36], the prediction errors in the control scheme are obtained by designing a new SPNEM. Third, the proposed command-filtered composite adaptive backstepping control scheme can achieve finite-time convergence of higher-order nonlinear systems. Different from existing control laws design in the backstepping procedure, a novel control law without singularity problem is designed at each step.

Remark 12: The design parameters of the proposed control scheme are usually selected according to the characteristics of the considered system and the range where the stability criteria are satisfied. For easy implementation, the selection principles of some important design parameters are provided. Note that all the parameters should be determined to ensure Theorem 1 holds. First, given that the nonsmooth term $\lceil \nu_i \rfloor^{\varrho}$ performs like a bridge between a discontinuous-feedback term ($\varrho = 0$) and a linear-feedback term ($\varrho = 1$) [59], one should select suitable ϱ to keep a balance between the robustness of the control system and the attenuation of chattering. Second, the control gains k_{i1} and k_{i2} should be set as large positive values to improve the convergence rate. Nevertheless, too large values of k_{i1} and k_{i2} will bring the problems of input saturation and energy waste. Thus, one should carefully make a tradeoff when choosing the control gains.

IV. Simulation Results

In this section, two examples will be given to illustrate the effectiveness and superiority of the proposed control scheme.

Example 1: To verify the effectiveness of the proposed control scheme, a second-order inverted pendulum system [60] is considered, whose dynamics is expressed as

$$\begin{cases} \dot{x}_1 = x_2 \\ \dot{x}_2 = \dfrac{g \sin x_1 - \frac{m_2 l x_2^2 \cos x_1 \sin x_1}{m_1 + m_2}}{l\left(\frac{4}{3} - \frac{m_2 \cos^2 x_1}{m_1 + m_2}\right)} \\ \qquad + \dfrac{\frac{\cos x_1}{m_1 + m_2}}{l\left(\frac{4}{3} - \frac{m_2 \cos^2 x_1}{m_1 + m_2}\right)} u + d_2 \\ y = x_1 \end{cases} \tag{61}$$

where x_1 denotes the angular position of the pendulum, x_2 denotes the corresponding angular velocity, m_1 denotes the mass of the cart, m_2 denotes the mass of the pendulum, l denotes the half length of the pendulum, d_2 denotes the external disturbance, and u denotes the applied force (control input). Besides, $g = 9.8\ \text{m/s}^2$ is the acceleration of gravity. In this example, we choose $m_1 = 1$ kg, $m_2 = 0.1$ kg, and $l = 0.5$ m. The parameters of the proposed control scheme are chosen as $k_{11} = 5$, $k_{12} = 2$, $k_{21} = 5$, $k_{22} = 2$, $\varrho = (9/11)$, $\xi_1 = \xi_2 = (1/2)$, $\tau_2 = (1/8)$, $\kappa_{21} = 2$, $\kappa_{22} = 1$, $\beta_2 = 5$, $\beta_{21} = 10$, and $\lambda_2 = 4$.

Scenario 1: The simulation in this scenario is conducted to demonstrate the effectiveness of the proposed control scheme. The reference signal is set as $y_d = 0.34\cos(0.58t+0.3)-0.26$. The initial values of $[x_1, x_2]^T$ are set as $[0.6, -0.2]^T$. The simulation results are shown in Figs. 2–4. Fig. 2 gives the tracking performance of the proposed control scheme. From it, we can see that the proposed control scheme obtains excellent tracking accuracy. Besides, the performance of the composite adaptive RBFNN $\hat{F}_2(\bar{x}_2) = W_2^T S_2$ is depicted in Fig. 3, which shows that the composite adaptive RBFNN $\hat{F}_2(\bar{x}_2)$ can approximate $F_2(\bar{x}_2)$ with high precision. In addition, the response curve of $\hat{x}_2$ is shown in Fig. 4, which verifies the effectiveness of the SPNEM and the composite adaptive RBFNN.

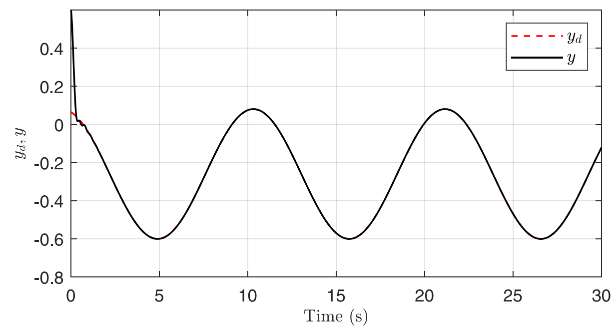

Fig. 2. Tracking performance of the proposed control scheme.

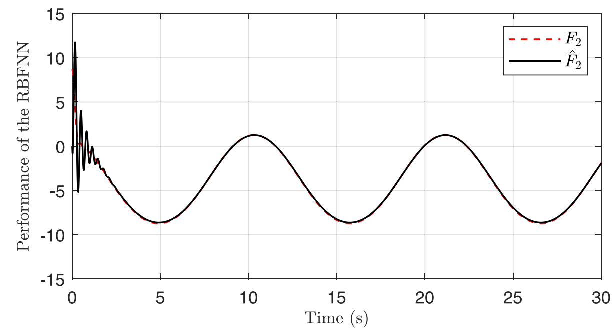

Fig. 3. Approximation result of F_2.

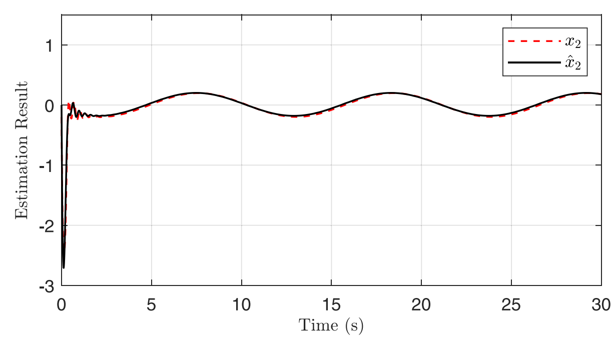

Fig. 4. Estimation result of the SPNEM.

Furthermore, in order to verify the superiority of the proposed control scheme in tracking precision, a comparative simulation is conducted. This simulation is carried out by applying the proposed control scheme given in Section III (denoted as "PCS" hereafter) and two comparative control schemes. The first comparative control scheme is the existing finite-time adaptive neural control scheme [45] (denoted as "EFCS" hereafter), which represents the improved version of the finite-time command-filtered control scheme in [45] by using conventional adaptive RBFNNs. Specifically, RBFNNs in the form of (6) are used to approximate the system unknown functions $F_i(\bar{x}_i)$ in (2). In addition, the adaptation law of EFCS is constructed as the traditional form: $\dot{W}_i = \beta_i \nu_i S_i - \sigma_i W_i$. The second comparative control scheme is the existing composite adaptive neural control scheme (denoted as "ECCS" hereafter), which is borrowed from [3] by replacing fuzzy systems with RBFNNs. To make a fair comparison, the three control schemes all adopt the same parameters. The tracking errors $e_1 = y - y_d$ by applying the three control schemes are shown

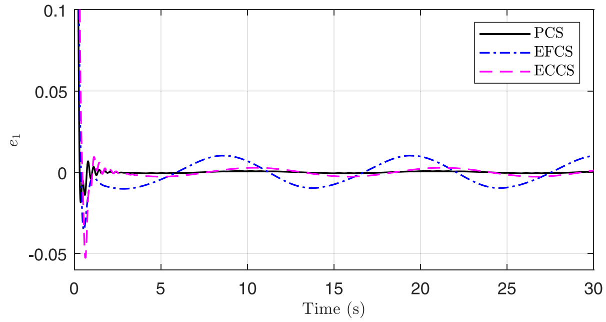

Fig. 5. Tracking errors by using the three control schemes.

TABLE I
QUANTITATIVE ASSESSMENT OF THE TRACKING PERFORMANCES FOR SCENARIO 1

Control Schemes	IAE	ITAE
PCS	0.1022	0.2010
EFCS	0.2902	2.8066
ECCS	0.1857	0.7859

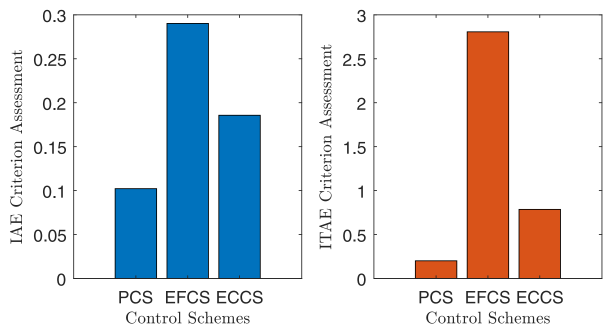

Fig. 6. Performance index comparisons in Scenario 1.

in Fig. 5. From it, we can observe that PCS obtains smaller tracking error than EFCS and ECCS. In addition, to evaluate the performances of the three control schemes, integral absolute error (IAE) and integral time absolute error (ITAE) are adopted as performance indices to quantify the tracking errors of these control schemes. IAE and ITAE are defined as $\int_0^T |e_1(t)|dt$ and $\int_0^T t|e_1(t)|dt$, respectively. The quantitative assessment results of the tracking performances are given in Table I and the performance index comparisons are illustrated in Fig. 6. These results clearly reveal that PCS outperforms EFCS and ECCS.

Scenario 2: In this simulation, the parameter uncertainties and external disturbances in the inverted pendulum dynamics (61) are both taken into consideration. To be more specific, all the coefficients of the nonlinear model (61) are chosen as 30% deviated from their nominal values and the external disturbance d_2 is set as $2\sin(t)+\cos(t)$ in the simulation model. In addition, we also apply PCS, EFCS, and ECCS to system (61). The comparative simulation results are shown in Figs. 7 and 8. IAE and ITAE are also adopted as performance indices to quantify the tracking errors of the three control schemes. The quantitative assessment results of the tracking performances are given in Table II and the performance index comparisons are illustrated in Fig. 9. From these results, we can clearly

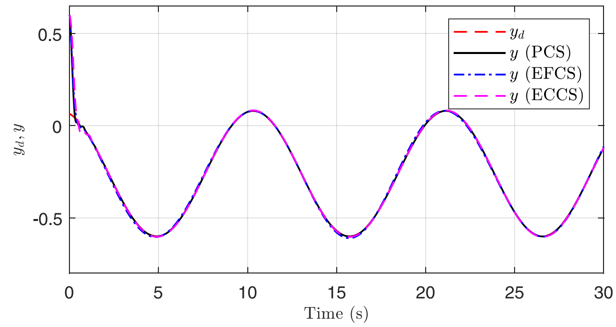

Fig. 7. Tracking performances of the three control schemes.

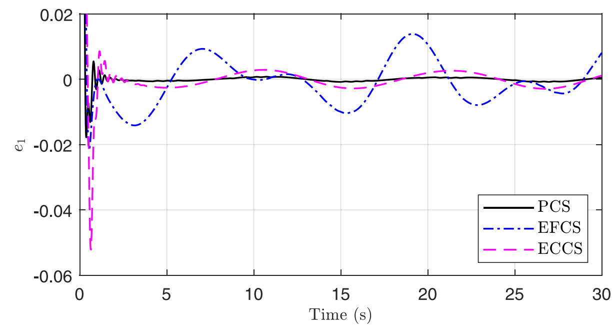

Fig. 8. Tracking errors by using the three control schemes.

TABLE II
QUANTITATIVE ASSESSMENT OF THE TRACKING PERFORMANCES FOR SCENARIO 2

Control Schemes	IAE	ITAE
PCS	0.1024	0.2089
EFCS	0.2589	2.2510
ECCS	0.1867	0.7980

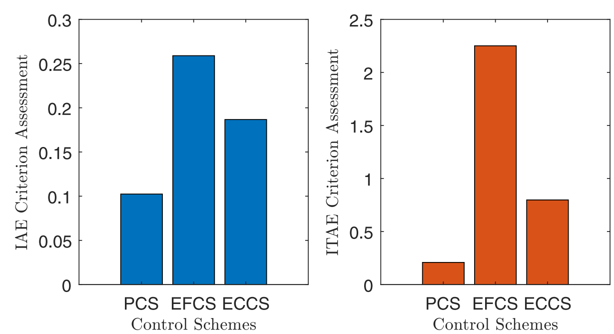

Fig. 9. Performance index comparisons in Scenario 2.

observe that PCS is superior to EFCS and ECCS in tracking precision.

Example 2: Inspired by the example in [45], we further consider the following third-order uncertain nonlinear system:

$$\begin{cases} \dot{x}_1 = x_2 \\ \dot{x}_2 = F_2(\bar{x}_2) + g_2(\bar{x}_2)x_3 + d_2 \\ \dot{x}_3 = F_3(\bar{x}_3) + g_3(\bar{x}_3)u + d_3 \\ y = x_1 \end{cases} \tag{62}$$

where $F_2(\bar{x}_2) = f_2(\bar{x}_2) + \Delta_2$, $F_3(\bar{x}_3) = f_3(\bar{x}_3) + \Delta_3$, $f_2(\bar{x}_2) = -32\sin(x_1) - 0.48x_2$, $g_2(\bar{x}_2) = 16$, $f_3(\bar{x}_3) = -0.06x_2 -$

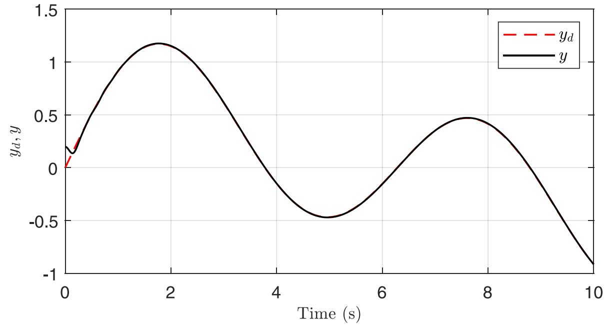

Fig. 10. Tracking performance of the proposed control scheme.

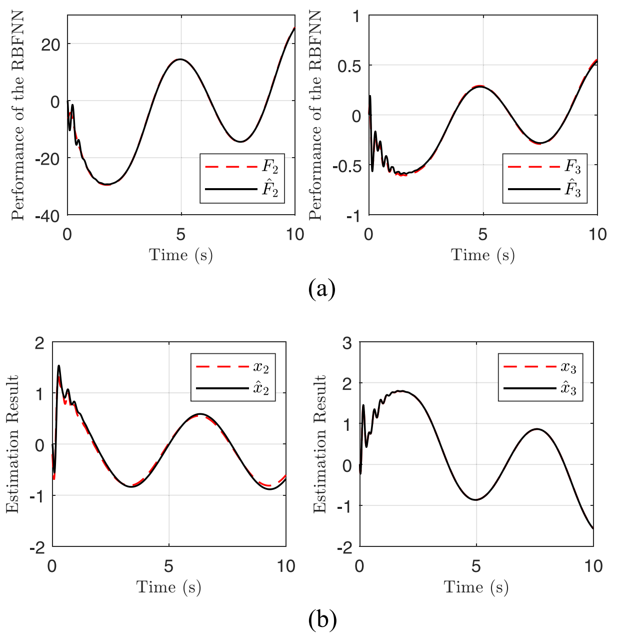

Fig. 11. Performances of the composite adaptive RBFNNs. (a) Approximation results of F_2 and F_3. (b) Estimation results of the SPNEMs.

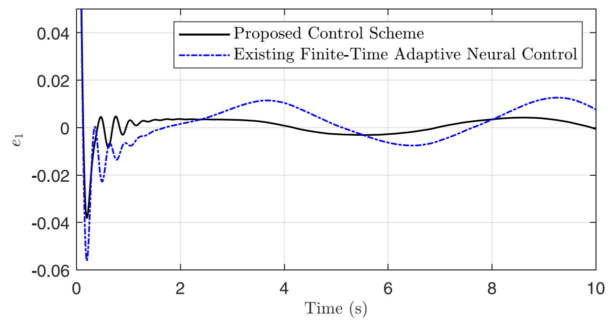

Fig. 12. Tracking errors by using two comparative control schemes.

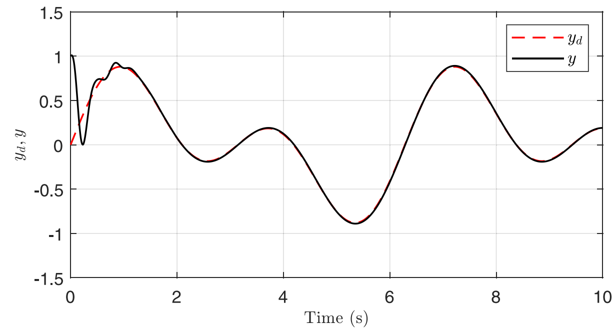

Fig. 13. Tracking performance of the proposed control scheme.

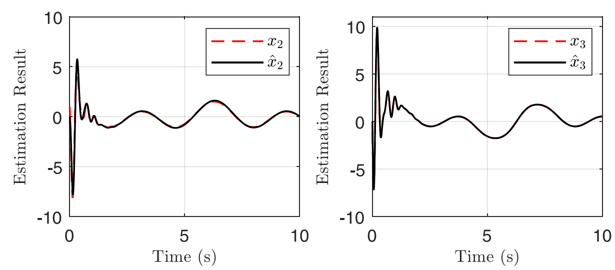

Fig. 14. Estimation results of the SPNEMs.

$(1/3)x_3$, and $g_3(\bar{x}_3) = (1/15)$. Besides,Δ_2 and Δ_3 denote the parameter uncertainties. Note that $F_2(\bar{x}_2)$ and $F_3(\bar{x}_3)$ are completely unknown for the control scheme design procedure. d_2, and d_3 represent the time-varying external disturbances.

The reference signal is set as $y_d = 0.8\sin(t) + 0.5\sin(0.5t)$. And the initial values of $[x_1, x_2, x_3]^T$ are set as $[0.2, -0.2, 0]^T$. The parameters of the proposed command-filtered composite adaptive neural control scheme are set as $k_{11} = 10$, $k_{12} = 2$, $k_{21} = 20$, $k_{22} = 2$, $k_{31} = 20$, $k_{32} = 2$, $\varrho = (9/11)$, $\xi_1 = \xi_2 = \xi_3 = (1/2)$, $\tau_2 = \tau_3 = (1/8)$, $\kappa_{21} = \kappa_{31} = 2$, $\kappa_{22} = \kappa_{32} = 1$, $\beta_2 = \beta_3 = 5$, $\beta_{21} = 5$, $\beta_{31} = 30$, and $\lambda_2 = \lambda_3 = 4$. Besides, there are two RBFNNs to approximate F_2 and F_3, and all the weights of the RBFNNs are initialized as zero.

The nominal simulation results are shown in Figs. 10 and 11. Fig. 10 shows the tracking performance of the proposed finite-time command-filtered composite adaptive neural control scheme. Clearly, the proposed control scheme guarantees that y tracks y_d in a rapid and precise way. In addition, the performances of the composite adaptive RBFNNs are depicted in Fig. 11. From Fig. 11(a), we can see that the composite adaptive RBFNNs $\hat{F}_2(\bar{x}_2) = W_2^T S_2$, $\hat{F}_3(\bar{x}_3) = W_3^T S_3$ can approximate $F_2(\bar{x}_2)$, $F_3(\bar{x}_3)$ with high accuracy. Besides, the estimation results of the SPNEMs, that is, the response curves of $\hat{x}_2$ and $\hat{x}_3$, are shown in Fig. 11(b), which further demonstrates the effectiveness of the composite adaptive RBFNNs.

Similar to Example 1, a comparative simulation between the proposed control scheme and the existing finite-time adaptive neural control scheme [45] is conducted. The simulation result is shown in Fig. 12. From it, a consistent conclusion can be obtained that the proposed control scheme can achieve better performance with smaller tracking error than the existing finite-time adaptive neural control scheme, which further verifies the superiority of the designed composite adaptation laws.

Furthermore, the robustness of the proposed composite adaptive neural control scheme is examined in the presence of parameter uncertainties and external disturbances. Specifically, all the coefficients of the nonlinear dynamic model (62) are chosen as 40% deviated from their nominal values and the external disturbances are set as $d_2 = 4\sin(t)$ and $d_3 =$

$2\sin(2t)$ in the simulation model. Besides, the initial values of $[x_1, x_2, x_3]^T$ are set as $[1, 1, -1]^T$, which lead to bigger initial tracking errors and estimation errors. In this case, the reference signal is chosen as $y_d = 0.5\sin(t) + 0.5\sin(2t)$. The simulation results are shown in Figs. 13 and 14. The tracking performance of the proposed command-filtered composite adaptive neural control scheme is shown in Fig. 13. Note that the precise values of F_2 and F_3 in (62) are hard to be depicted when the model is exposed to parameter uncertainties. Thus, the approximation performances of the composite adaptive RBFNNs are illustrated by observing the estimation results of the SPNEMs in Fig. 14. From Fig. 14, it is inferred that the composite adaptive RBFNNs can still approximate the unknown functions F_2 and F_3 effectively. From these results, we can conclude that the proposed control scheme still achieves satisfactory performance when the nonlinear dynamic model (62) is exposed to various parameter uncertainties and external disturbances.

V. Conclusion

This article has proposed a novel command-filtered composite adaptive neural control scheme for uncertain nonlinear systems with finite-time convergence. By constructing the prediction errors from the SPNEMs, the prediction errors and tracking errors are utilized together to design the composite adaptation laws for updating RBFNN weights. The ANDOs are designed to compensate for the external disturbances and RBFNN minimum approximation errors. Subsequently, the overall control scheme design is accomplished by using the nonsmooth command-filtered backstepping technique. The proposed control scheme is featured with many advantages. First, the scheme guarantees that high precision tracking performances and NN approximation performances can be achieved simultaneously. Second, the scheme greatly improves the robustness of the control system by compensating the lumped disturbances. Third, the scheme ensures finite-time convergence of all signals in the closed-loop system. The future works will be focused on reducing the parameters of the proposed control scheme via minimal-learning-parameter technique and designing finite-time convergent composite adaptive control schemes for uncertain nonlinear systems with full-state constraints.

References

[1] M. Chen, P. Shi, and C.-C. Lim, "Robust constrained control for MIMO nonlinear systems based on disturbance observer," *IEEE Trans. Autom. Control*, vol. 60, no. 12, pp. 3281–3286, Dec. 2015.

[2] C. L. P. Chen, G.-X. Wen, Y.-J. Liu, and Z. Liu, "Observer-based adaptive backstepping consensus tracking control for high-order nonlinear semi-strict-feedback multiagent systems," *IEEE Trans. Cybern.*, vol. 46, no. 7, pp. 1591–1601, Jul. 2016.

[3] B. Xu and F. Sun, "Composite intelligent learning control of strict-feedback systems with disturbance," *IEEE Trans. Cybern.*, vol. 48, no. 2, pp. 730–741, Feb. 2018.

[4] X. Cao, P. Shi, Z. Li, and M. Liu, "Neural-network-based adaptive backstepping control with application to spacecraft attitude regulation," *IEEE Trans. Neural Netw. Learn. Syst.*, vol. 29, no. 9, pp. 4303–4313, Sep. 2018.

[5] Y.-H. Jing and G.-H. Yang, "Adaptive fuzzy output feedback fault-tolerant compensation for uncertain nonlinear systems with infinite number of time-varying actuator failures and full-state constraints," *IEEE Trans. Cybern.*, early access, Mar. 29, 2019, doi: 10.1109/TCYB.2019.2904768.

[6] K. Zhang, B. Jiang, X.-G. Yan, Z. Mao, and M. M. Polycarpou, "Fault-tolerant control for systems with unmatched actuator faults and disturbances," *IEEE Trans. Autom. Control*, early access, May 25, 2020, doi: 10.1109/TAC.2020.2997347.

[7] D. Swaroop, J. K. Hedrick, P. P. Yip, and J. C. Gerdes, "Dynamic surface control for a class of nonlinear systems," *IEEE Trans. Autom. Control*, vol. 45, no. 10, pp. 1893–1899, Oct. 2000.

[8] J. A. Farrell, M. Polycarpou, M. Sharma, and W. Dong, "Command filtered backstepping," *IEEE Trans. Autom. Control*, vol. 54, no. 6, pp. 1391–1395, Jun. 2009.

[9] J. Yu, P. Shi, C. Lin, and H. Yu, "Adaptive neural command filtering control for nonlinear MIMO systems with saturation input and unknown control direction," *IEEE Trans. Cybern.*, vol. 50, no. 6, pp. 2536–2545, Jun. 2020, doi: 10.1109/TCYB.2019.2901250.

[10] Y.-J. Liu, S. Lu, S. Tong, X. Chen, C. L. P. Chen, and D.-J. Li, "Adaptive control-based Barrier Lyapunov functions for a class of stochastic nonlinear systems with full state constraints," *Automatica*, vol. 87, pp. 83–93, Jan. 2018.

[11] X. Zheng and X. Yang, "Command filter and universal approximator based backstepping control design for strict-feedback nonlinear systems with uncertainty," *IEEE Trans. Autom. Control*, vol. 65, no. 3, pp. 1310–1317, Mar. 2020.

[12] J. Sun, J. Yang, S. Li, and W. X. Zheng, "Sampled-data-based event-triggered active disturbance rejection control for disturbed systems in networked environment," *IEEE Trans. Cybern.*, vol. 49, no. 2, pp. 556–566, Feb. 2019.

[13] Y. Cui, H. Zhang, Y. Wang, and H. Jiang, "A fuzzy adaptive tracking control for MIMO switched uncertain nonlinear systems in strict-feedback form," *IEEE Trans. Fuzzy Syst.*, vol. 27, no. 12, pp. 2443–2452, Dec. 2019.

[14] Y.-X. Li, S. Tong, and G.-H. Yang, "Observer-based adaptive fuzzy decentralized event-triggered control of interconnected nonlinear system," *IEEE Trans. Cybern.*, vol. 50, no. 7, pp. 3104–3112, Jul. 2019, doi: 10.1109/TCYB.2019.2894024.

[15] J. Dong, Y. Wu, and G.-H. Yang, "A new sensor fault isolation method for T–S fuzzy systems," *IEEE Trans. Cybern.*, vol. 47, no. 9, pp. 2437–2447, Sep. 2017.

[16] H. Wang, P. X. Liu, S. Li, and D. Wang, "Adaptive neural output-feedback control for a class of nonlower triangular nonlinear systems with unmodeled dynamics," *IEEE Trans. Neural Netw. Learn. Syst.*, vol. 29, no. 8, pp. 3658–3668, Aug. 2018.

[17] S. Wen, M. Z. Q. Chen, Z. Zeng, T. Huang, and C. Li, "Adaptive neural-fuzzy sliding-mode fault-tolerant control for uncertain nonlinear systems," *IEEE Trans. Syst., Man, Cybern., Syst.*, vol. 47, no. 8, pp. 2268–2278, Aug. 2017.

[18] D. Zhao, Q. Zhang, D. Wang, and Y. Zhu, "Experience replay for optimal control of nonzero-sum game systems with unknown dynamics," *IEEE Trans. Cybern.*, vol. 46, no. 3, pp. 854–865, Mar. 2016.

[19] B. Xu, R. Zhang, S. Li, W. He, and Z. Shi, "Composite neural learning-based nonsingular terminal sliding mode control of MEMS gyroscopes," *IEEE Trans. Neural Netw. Learn. Syst.*, vol. 31, no. 4, pp. 1375–1386, Apr. 2020, doi: 10.1109/TNNLS.2019.2919931.

[20] H. Sun, L. Hou, G. Zong, and X. Yu, "Adaptive decentralized neural network tracking control for uncertain interconnected nonlinear systems with input quantization and time delay," *IEEE Trans. Neural Netw. Learn. Syst.*, vol. 31, no. 4, pp. 1401–1409, Apr. 2020.

[21] K. Zhang, H. Zhang, Z. Gao, and H. Su, "Online adaptive policy iteration based fault-tolerant control algorithm for continuous-time nonlinear tracking systems with actuator failures," *J. Franklin Inst.*, vol. 355, no. 15, pp. 6947–6968, 2018.

[22] B. Xu, C. Yang, and Z. Shi, "Reinforcement learning output feedback NN control using deterministic learning technique," *IEEE Trans. Neural Netw. Learn. Syst.*, vol. 25, no. 3, pp. 635–641, Mar. 2014.

[23] M. Chen, S.-Y. Shao, and B. Jiang, "Adaptive neural control of uncertain nonlinear systems using disturbance observer," *IEEE Trans. Cybern.*, vol. 47, no. 10, pp. 3110–3123, Oct. 2017.

[24] W. He, Y. Sun, Z. Yan, C. Yang, Z. Li, and O. Kaynak, "Disturbance observer-based neural network control of cooperative multiple manipulators with input saturation," *IEEE Trans. Neural Netw. Learn. Syst.*, vol. 31, no. 5, pp. 1735–1746, May 2020, doi: 10.1109/TNNLS.2019.2923241.

[25] D.-P. Li, Y.-J. Liu, S. Tong, C. L. P. Chen, and D.-J. Li, "Neural networks-based adaptive control for nonlinear state constrained systems with input delay," *IEEE Trans. Cybern.*, vol. 49, no. 4, pp. 1249–1258, Apr. 2019.

[26] F. L. Lewis, S. Jagannathan, and A. Yesildirak, *Neural Network Control of Robot Manipulators and Nonlinear Systems*. London, U.K.: Taylor & Francis, 1999.

[27] H. Sun, G. Zong, and C. K. Ahn, "Quantized decentralized adaptive neural network PI tracking control for uncertain interconnected nonlinear systems with dynamic uncertainties," *IEEE Trans. Syst., Man, Cybern., Syst.*, early access, Jun. 13, 2019, doi: 10.1109/TSMC.2019.2918142.

[28] H. Wang, P. X. Liu, J. Bao, X.-J. Xie, and S. Li, "Adaptive neural output-feedback decentralized control for large-scale nonlinear systems with stochastic disturbances," *IEEE Trans. Neural Netw. Learn. Syst.*, vol. 31, no. 3, pp. 972–983, Mar. 2020.

[29] B. Xu, Z. Shi, C. Yang, and F. Sun, "Composite neural dynamic surface control of a class of uncertain nonlinear systems in strict-feedback form," *IEEE Trans. Cybern.*, vol. 44, no. 12, pp. 2626–2634, Dec. 2014.

[30] S.-L. Dai, S. He, M. Wang, and C. Yuan, "Adaptive neural control of underactuated surface vessels with prescribed performance guarantees," *IEEE Trans. Neural Netw. Learn. Syst.*, vol. 30, no. 12, pp. 3686–3698, Dec. 2019.

[31] W. He, Z. Yan, Y. Sun, Y. Ou, and C. Sun, "Neural-learning-based control for a constrained robotic manipulator with flexible joints," *IEEE Trans. Neural Netw. Learn. Syst.*, vol. 29, no. 12, pp. 5993–6003, Dec. 2018.

[32] H. Wang, P. Shi, H. Li, and Q. Zhou, "Adaptive neural tracking control for a class of nonlinear systems with dynamic uncertainties," *IEEE Trans. Cybern.*, vol. 47, no. 10, pp. 3075–3087, Oct. 2017.

[33] T. Sun, L. Peng, L. Cheng, Z.-G. Hou, and Y. Pan, "Composite learning enhanced robot impedance control," *IEEE Trans. Neural Netw. Learn. Syst.*, vol. 31, no. 3, pp. 1052–1059, Mar. 2020.

[34] B. Xu, "Composite learning control of flexible-link manipulator using NN and DOB," *IEEE Trans. Syst., Man, Cybern., Syst.*, vol. 48, no. 11, pp. 1979–1985, Nov. 2018.

[35] Y. Li, S. Tong, and T. Li, "Composite adaptive fuzzy output feedback control design for uncertain nonlinear strict-feedback systems with input saturation," *IEEE Trans. Cybern.*, vol. 45, no. 10, pp. 2299–2308, Oct. 2015.

[36] L. Wang, M. V. Basin, H. Li, and R. Lu, "Observer-based composite adaptive fuzzy control for nonstrict-feedback systems with actuator failures," *IEEE Trans. Fuzzy Syst.*, vol. 26, no. 4, pp. 2336–2347, Aug. 2018.

[37] S. P. Bhat and D. S. Bernstein, "Finite-time stability of continuous autonomous systems," *SIAM J. Control Optim.*, vol. 38, no. 3, pp. 751–766, 2000.

[38] H. Du, S. Li, and C. Qian, "Finite-time attitude tracking control of spacecraft with application to attitude synchronization," *IEEE Trans. Autom. Control*, vol. 56, no. 11, pp. 2711–2717, Nov. 2011.

[39] B. Tian, H. Lu, Z. Zuo, and W. Yang, "Fixed-time leader–follower output feedback consensus for second-order multiagent systems," *IEEE Trans. Cybern.*, vol. 49, no. 4, pp. 1545–1550, Apr. 2019.

[40] L. Wang, Z. Zeng, and M.-F. Ge, "A disturbance rejection framework for finite-time and fixed-time stabilization of delayed memristive neural networks," *IEEE Trans. Syst., Man, Cybern., Syst.*, early access, Jan. 3, 2019, doi: 10.1109/TSMC.2018.2888867.

[41] S. Ding, K. Mei, and S. Li, "A new second-order sliding mode and its application to nonlinear constrained systems," *IEEE Trans. Autom. Control*, vol. 64, no. 6, pp. 2545–2552, Jun. 2019.

[42] H. Zhang, J. Duan, Y. Wang, and Z. Gao, "Bipartite fixed-time output consensus of heterogeneous linear multiagent systems," *IEEE Trans. Cybern.*, early access, Sep. 6, 2019, doi: 10.1109/TCYB.2019.2936009.

[43] Z. Gao, H. Zhang, J. Duan, and Y. Cai, "Guaranteed-performance consensus for descriptor nonlinear multi-agent systems based on distributed nonlinear consensus protocol," *Neurocomputing*, vol. 383, pp. 359–367, Mar. 2020.

[44] W. Qi, G. Zong, and H. R. Karimi, "Finite-time observer-based sliding mode control for quantized Semi-Markov switching systems with application," *IEEE Trans. Ind. Informat.*, vol. 16, no. 2, pp. 1259–1271, Feb. 2020.

[45] J. Yu, P. Shi, and L. Zhao, "Finite-time command filtered backstepping control for a class of nonlinear systems," *Automatica*, vol. 92, pp. 173–180, Jun. 2018.

[46] F. Wang, B. Chen, C. Lin, J. Zhang, and X. Meng, "Adaptive neural network finite-time output feedback control of quantized nonlinear systems," *IEEE Trans. Cybern.*, vol. 48, no. 6, pp. 1839–1848, Jun. 2018.

[47] Y. Sun, B. Chen, C. Lin, and H. Wang, "Finite-time adaptive control for a class of nonlinear systems with nonstrict feedback structure," *IEEE Trans. Cybern.*, vol. 48, no. 10, pp. 2774–2782, Oct. 2018.

[48] L. Zhao, J. Yu, C. Lin, and Y. Ma, "Adaptive neural consensus tracking for nonlinear multiagent systems using finite-time command filtered backstepping," *IEEE Trans. Syst., Man, Cybern., Syst.*, vol. 48, no. 11, pp. 2003–2012, Nov. 2018.

[49] H. Wang, P. X. Liu, X. Zhao, and X. Liu, "Adaptive fuzzy finite-time control of nonlinear systems with actuator faults," *IEEE Trans. Cybern.*, vol. 50, no. 5, pp. 1786–1797, May 2020.

[50] F. Wang, B. Chen, X. Liu, and C. Lin, "Finite-time adaptive fuzzy tracking control design for nonlinear systems," *IEEE Trans. Fuzzy Syst.*, vol. 26, no. 3, pp. 1207–1216, Jun. 2018.

[51] Y.-X. Li, "Finite time command filtered adaptive fault tolerant control for a class of uncertain nonlinear systems," *Automatica*, vol. 106, pp. 117–123, Aug. 2019.

[52] W.-H. Chen, J. Yang, L. Guo, and S. Li, "Disturbance-observer-based control and related methods—An overview," *IEEE Trans. Ind. Electron.*, vol. 63, no. 2, pp. 1083–1095, Feb. 2016.

[53] H. Ren, G. Zong, and H. R. Karimi, "Asynchronous finite-time filtering of networked switched systems and its application: An event-driven method," *IEEE Trans. Circuits Syst. I, Reg. Papers*, vol. 66, no. 1, pp. 391–402, Jan. 2019.

[54] S. Yu, X. Yu, B. Shirinzadeh, and Z. Man, "Continuous finite-time control for robotic manipulators with terminal sliding mode," *Automatica*, vol. 41, no. 11, pp. 1957–1964, Nov. 2005.

[55] X. Jin, "Adaptive finite-time fault-tolerant tracking control for a class of MIMO nonlinear systems with output constraints," *Int. J. Robust Nonlinear Control*, vol. 27, no. 5, pp. 722–741, 2017.

[56] G. H. Hardy, J. E. Littlewood, and G. Polya, *Inequalities*. Cambridge, U.K.: Cambridge Univ. Press, 1952.

[57] S. Sui, C. L. P. Chen, and S. Tong, "Fuzzy adaptive finite-time control design for nontriangular stochastic nonlinear systems," *IEEE Trans. Fuzzy Syst.*, vol. 27, no. 1, pp. 172–184, Jan. 2019.

[58] G. Zong, Y. Li, and H. Sun, "Composite anti-disturbance resilient control for Markovian jump nonlinear systems with general uncertain transition rate," *Sci. China Inf. Sci.*, vol. 62, no. 2, 2019, Art. no. 22205.

[59] Z. Wang, S. Li, J. Yang, and Q. Li, "Current sensorless finite-time control for buck converters with time-varying disturbances," *Control Eng. Pract.*, vol. 77, pp. 127–137, Aug. 2018.

[60] H. Li, S. Zhao, W. He, and R. Lu, "Adaptive finite-time tracking control of full state constrained nonlinear systems with dead-zone," *Automatica*, vol. 100, pp. 99–107, Feb. 2019.

Jinlin Sun received the B.Eng. degree in automation from Jiangsu University, Zhenjiang, China, in 2016. He is currently pursuing the Ph.D. degree in control theory and control engineering with the Institute of Automation, Chinese Academy of Sciences, Beijing, China.

He is also currently a visiting student with the Department of Electrical, Computer, and Biomedical Engineering, University of Rhode Island, Kingston, RI, USA. His current research interests include robust adaptive control and finite-time control.

Haibo He (Fellow, IEEE) received the B.S. and M.S. degrees in electrical engineering from the Huazhong University of Science and Technology, Wuhan, China, in 1999 and 2002, respectively, and the Ph.D. degree in electrical engineering from Ohio University, Athens, OH, USA, in 2006.

From 2006 to 2009, he was an Assistant Professor with the Department of Electrical and Computer Engineering, Stevens Institute of Technology, Hoboken, NJ, USA. He is currently the Robert Haas Endowed Chair Professor with the Department of Electrical, Computer, and Biomedical Engineering, University of Rhode Island, Kingston, RI, USA.

Dr. He was a recipient of the IEEE International Conference on Communications Best Paper Award in 2014, the IEEE Computational Intelligence Society Outstanding Early Career Award in 2014, and the National Science Foundation CAREER Award in 2011. He served as the General Chair of the IEEE Symposium Series on Computational Intelligence in 2014. He is currently the Editor-in-Chief of the IEEE Transactions on Neural Networks and Learning Systems.

Jianqiang Yi (Senior Member, IEEE) received the B.Eng. degree in mechanical engineering from the Beijing Institute of Technology, Beijing, China, in 1985, and the M.Eng. and Ph.D. degrees in automation from the Kyushu Institute of Technology, Kitakyushu, Japan, in 1989 and 1992, respectively.

From 1992 to 1994, he worked as a Research Fellow with Computer Software Development Company, Tokyo, Japan. From 1994 to 2001, he was a Chief Engineer with MYCOM, Inc., Kyoto, Japan. Since 2001, he has been a Full Professor with the Institute of Automation, Chinese Academy of Sciences, Beijing. He has authored or coauthored over 100 international journal papers and 240 international conference papers. He holds more than 40 issued domestic patents. His research interests mainly include intelligent control and adaptive control.

Prof. Yi was an Associate Editor of *IEEE Computational Intelligence Magazine* from 2008 to 2009, and is an Associate Editor of the *Journal of Advanced Computational Intelligence*, *Intelligent Informatics*, *International Journal of Innovative Computing*, and *Information and Control*.

Zhiqiang Pu received the B.Eng. degree in automation from Wuhan University, Wuhan, China, in 2009, and the Ph.D. degree in control theory and control engineering from the Institute of Automation, Chinese Academy of Sciences, Beijing, China, in 2014.

He is currently an Associate Professor with the Integrated Information System Research Center, Institute of Automation, Chinese Academy of Sciences. He has been supported by the Talent Program of Youth Innovation Promotion Association, Chinese Academy of Sciences, since 2017. His current research interests mainly include nonlinear control and robust adaptive control.